IET Generation, Transmission & Distribution

Research Article

IET Journals
The Institution of Engineering and Technology

Intentional power system islanding under cascading outages using energy function method

ISSN 1751-8687
Received on 4th March 2019
Revised 6th July 2020
Accepted on 14th July 2020
E-First on 3rd September 2020
doi: 10.1049/iet-gtd.2019.0317
www.ietdl.org

Sadegh Kamali[1], Turaj Amraee[1] ✉, Mojdeh Khorsand[2]

[1]*Faculty of Electrical Engineering, K. N. Toosi University of Technology, Tehran, Iran*
[2]*School of Electrical, Computer, and Energy Engineering, Arizona State University, Tempe, AZ, USA*
✉ *E-mail: amraee@kntu.ac.ir*

Abstract: In this study, the 'where to island' issue under the transient stability constraints is addressed. Without considering the transient stability, the islanding strategy may fail to stop the propagation of harmful dynamics throughout the network. This study promotes the current available controlled islanding model to handle the transient stability criteria, which is the most important issue during network splitting. Based on the wide area measurements, a two-stage transient stability constrained network splitting model is developed using a proper transient energy function. In the first stage, the conventional intentional splitting problem is formulated as a mixed-integer linear programming (MILP) optimisation model with considering operational, coherency and linear AC load flow constraints. The boundary of each island is determined using an optimisation model to achieve the minimum total power imbalance. To assess the transient stability, the network splitting plan obtained from the first stage is then evaluated in the second stage using a transient energy function. In the second stage, to satisfy the transient stability constraint of the critical island, a linear constraint is constructed and added to the MILP formulation of the first stage. In the second stage, the saddle or control unstable equilibrium points are determined using an optimisation model.

Nomenclature

Parameters

$\Delta P_{\mathrm{e}}^{t}$	real time electrical power changes
Bu_{ij}	auxiliary binary parameter
I_g	non-square identity matrix
$P_{\mathrm{e}i}/P_{\mathrm{m}i}$	electrical/mechanical power of generator i
E_i	internal voltage of generator i
M_i	inertia moment of generator i
N_{b}	number of all nodes
N_{g}	number of generating units
N_{l}	number of load points
$En_{\mathrm{k}}/En_{\mathrm{p}}$	kinetic/potential energy
$P_{\mathrm{l}_i}/Q_{\mathrm{l}_i}$	active/reactive load powers at bus i
L	large positive arbitrary number
$\alpha_{lm}^{(k)}$	control factor to limit the transfer impedance between generators l and m
γ	threshold of relative mechanical torque
$\varnothing_{i,j}$	angle of transfer impedance between generators i and j
ω_i	rotor speed of generator i
$\omega_{i,j}^{\mathrm{R}}$	real time estimated speed of generator i w.r.t. j
$Z_{ij}^{\mathrm{c}}/Z_{ij}^{\mathrm{is}}$	transfer impedance between generator i and j in connected/islanded network
$\delta_{i,j}^{\mathrm{R}}$	real-time rotor angle between generator i and j

Sets

Ω^{d}	set of load points
Ω^{g}	set of generating units
Ω_{ns}^{g}	set of generators in island ns
Ω^{l}	set of transmission lines

Variables

$GL_{i,j}^{\mathrm{new}}/BL_{i,j}^{\mathrm{new}}$	conductance /susceptance between nodes i and j
Su_{ij}	auxiliary binary variable for linearisation
P_{ij}	power flow across line between nodes i and j
$\Delta P_{e_i}^{+}$	decelerating power
$\Delta P_{e_i}^{-}$	accelerating power
$Q_{\mathrm{G}i}$	reactive power output of generating unit i
U_{ij}	open/close status of candidate transmission line between nodes i and j
V_i	voltage magnitude of bus i
Z_{ij}	transfer impedance between generators i and j
θ_i	voltage angle of bus i
$\delta_{i,j}$	rotor angle between generators i and j
$\delta_{i,j}^{s(k)}$	saddle point between generators i and j at iteration k
$\delta_{i,j}^{\mathrm{sep}}$	stable equilibrium point between units i and j at iteration k

1 Introduction

Cascading events are a major threat to the integrity and interconnectivity of power systems. Although the cascading failures or blackouts are rare events, they significantly impact the economy and society due to their serious consequences [1, 2]. Usually, such extreme events happen when the system is heavily loaded, and a few unplanned or forced outages occur within short time intervals [3].

During cascading failures, formation of the coherent groups of generators is expected. The weak connections between non-coherent groups of generators may facilitate the propagation of fast and harmful dynamics. Controlled or intentional islanding is the last remedial action against the unwanted electrical separation of non-coherent groups of generators. Two independent issues including where and when to island are addressed in controlled islanding scheme [4]. The focus of the present paper is to determine the islanding boundary (i.e. where to island) considering the transient stability constraint. Although, the steady-state operational constraints such as power balance in resulted islands are of great importance, a major prerequisite for the success of any controlled islanding scheme is the preservation of rotor angle transient stability constraint. The detailed definition and

classification of stability phenomenon including the rotor angle transient stability can be found in [5].

Different approaches including the slow coherency technique, graph-based techniques and optimisation methods have been developed to determine the islanding boundary (i.e. where to island issue).

According to the coherency criterion, the coherent group of generators must remain in the same island. In [6, 7], the set of coherent groups of generators are determined based on the wide area measurements. Then, the islanding boundaries are determined to provide the minimum power imbalance in each island. A major challenge in coherency-based islanding is the online detection of coherent groups that has been investigated in [8–10]. Coherency can be used for detecting weak connections between different electric areas of the power system. For this reason, coherency technique is used for intentional islanding of the power system under emergency conditions [11]. The slow coherency method has been applied to Western Electricity Coordinating Council (WECC) system in [12].

In order to reduce the structural complexity of large power systems, the slow coherency technique may be promoted using the graph-based techniques [12–15]. In this method, buses and transmission lines are considered as vertices and edges, respectively. In [16–19], the ordinary binary decision diagram technique is proposed for proper splitting, with considering the necessary steady-state operational constraints of the resulted islands. Also this method has been applied in WECC system [20].

Using the optimisation-based islanding method, the islanding boundary (i.e. the set of transmission lines or the splitting points) may be determined to achieve the minimum power imbalance over the resulted islands. In optimisation-based islanding methods, all the required operational constraints (e.g. power balance of resulted islands, transmission limits etc.) and structural constraints (e.g. connectivity of coherent generators in each island, disconnectivity of non-coherent generators etc.) are integrated in an optimisation model. In [21, 22], the set of splitting lines are determined using a mixed-integer linear programming (MILP) model. In [23], the efficacy of the optimisation based controlled islanding model has been promoted using a graph-based approach. The proposed model in [24] is able to maintain the voltage magnitudes within an acceptable range. Also, the same approach with considering the DC power flow has been presented in [25].

It is evident that during the intentional network splitting, there is a significant risk of transient instability. Indeed, although the previously proposed models determine the islanding boundaries considering power imbalance [4, 6, 7, 12–15, 21, 23] and/or frequency stability criterion [26, 27], the resulted splitting solution might still be at risk of transient instability. Since the direct transient stability assessment methods allow the analytic calculation of the transient stability margin [28], this paper presents a new analytic model considering a novel transient stability constraint using a transient energy function (TEF). The efficacy of the TEF method in transient stability assessment is investigated in [29–31]. In other words, the gap that this paper intends to fill is the integration of the transient stability constraint in controlled islanding model using a direct energy function method.

The main salient contributions of this paper can be summarised as follows:

(i) Proposing an intentional islanding model against the cascading failures with preserving the transient stability of the resulted islands. The proposed method promotes the steady-state islanding models to consider the transient stability under the network splitting.
(ii) Proposing an analytical linear transient stability constraint using TEF method without any need to further time-domain simulation. The proposed method gives a transient-stable islanding plan avoiding time-consuming simulations.
(iii) Constructing an MILP formulation for the developed transient stability constrained intentional splitting model. The optimal islanding solution is obtained by solving the proposed MILP model.
(iv) Wide area measurements are used to cope the proposed islanding model with the actual operational conditions of the system. These measurements are used in different parts of the proposed method.

The rest of this paper is organised as follows. In Section 2, the overall structure of the developed islanding scheme is presented. The proposed MIP islanding model is presented in Section 3. Also, the detailed formulation of the transient stability function and finding saddle point is described in Section 4. Linear constraint is constructed based on energy function concept in Section 5. In Section 6, the proposed model is applied on the IEEE 118-bus test case. Simulation results are given in Section 7. Finally, the paper is concluded in Section 8.

2 Overall structure of the proposed method

The overall structure of the proposed transient stability constrained islanding model has been illustrated in Fig. 1. It is assumed that the issue of 'when to island' is decided using an islanding prediction algorithm such as the method proposed in [4, 32]. This paper addresses the 'where to island' issue to determine the splitting boundary. The measurement data from the wide area measurement system (WAMS), including but not limited to network topology, are the input of the first stage (i.e. MILP-only islanding model). The proposed method might be used near to real-time provided that the required inputs are known at the right time. Practically, the candidate splitting points are limited to inter-area transmission lines and the developed model may be run in a reasonable time. The requirements for online and offline applications of controlled islanding schemes such as selecting candidate lines, can be found in [33]. The splitting strategy obtained from the MILP model of the first stage is then passed to the second stage, where the TEF is constructed to assess the transient stability of the network under the given islanding strategy. The proposed TEF needs the saddle points of each island. To this end, the saddle or control unstable equilibrium points (CUEPs) are determined in this stage. According to the developed TEF, if the transient stability criterion is met, the iterative process between the first and second stages is stopped, otherwise based on the most sensitive splitting lines a linear constraint is constructed and returned to the MILP model of the first stage. A procedure is presented to determine the most sensitive splitting lines. This iterative process continues until the stability criterion is ultimately satisfied.

The proposed controlled islanding can be performed near to real time using phasor measurement unit (PMU) measurements, i.e. active power and voltage phasors at generators' terminals, which are transmitted to the energy management system centre via the WAMS infrastructure. To this end, the internal voltages of generators can be estimated based on the following equation:

$$E_i\angle\delta_i = V_i\angle\theta_i - Z_{gi} \times \frac{P_{ei} - jQ_{ei}}{V_i\angle - \theta_i} \tag{1}$$

One input parameter of the MILP-based controlled islanding plan is the input mechanical power of each generator that can be determined by measuring the electrical power outputs of generators. During transient regime, the input mechanical power of a given generator is approximately constant. Without loss of generality, in this paper, it is assumed that the mechanical power of each generator is an input parameter and is known based on the measured electrical power output of that generator.

3 First stage: the proposed MILP islanding model

In the first stage, the set of splitting lines is determined without considering the transient stability constraint. In order to reduce the computational burden, the mixed integer non-linear programming model of controlled islanding is converted to a MILP model. The objective function, operational constraints including the linear AC power balance model, the coherency-based grouping of generators and the connectivity constraint in each island are presented in the following.

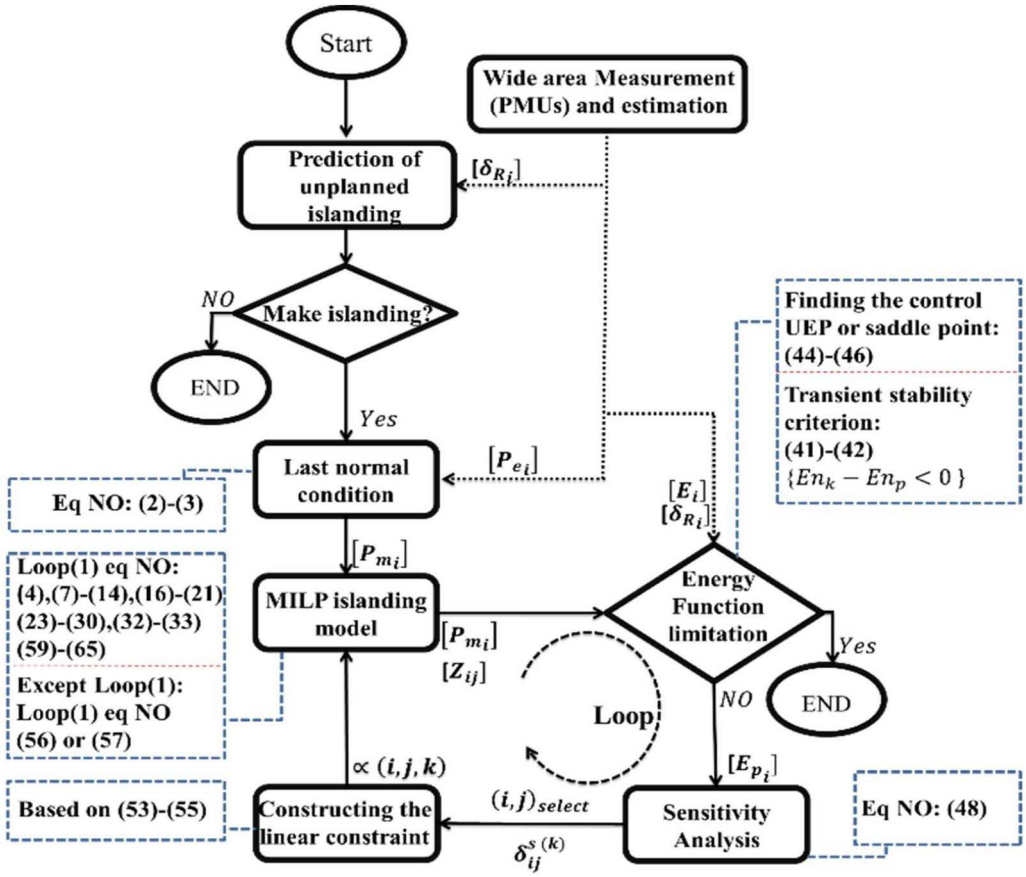

Fig. 1 *Overall structure of the proposed TEF-based two-stage model*

- The objective function

Conventionally, the islanding strategy should split the network such that the power balance in all resulted islands is fulfilled with minimum load and generation shedding. The objective function of the proposed model is defined to minimise the total power imbalance as follows:

$$\mathrm{PI} = \sum_{i=1}^{N_g} (\Delta P_{e_i}^- + \Delta P_{e_i}^+) \tag{2}$$

3.1 Constraints

A variety of constraints including power balance, operational limits, coherency-based grouping of generators and connectivity of each island may be considered in the optimisation model of islanding in the first stage as follows.

- Power balance

The non-linear active and reactive AC power balance equations for all buses (i.e. $i = 1, \ldots, N_b$), considering the power imbalance resulted by the network splitting are expressed as below:

$$\begin{aligned}&\left[P_{gi}^0 + \Delta P_{e_i}^+ - \Delta P_{e_i}^- - P_{li}\right] \\ &= V_i \sum_{j=1}^{N_b} V_j \left(GL_{ij}^{new}\cos(\theta_i - \theta_j) + BL_{ij}^{new}\sin(\theta_i - \theta_j)\right)\end{aligned} \tag{3}$$

$$\begin{aligned}&[Q_{Gi} - Q_{Li}] \\ &= V_i \sum_{j=1}^{N_b} V_j \left(GL_{ij}^{new}\sin(\theta_i - \theta_j) - BL_{ij}^{new}\cos(\theta_i - \theta_j)\right)\end{aligned} \tag{4}$$

The decision variables of the controlled islanding scheme are the open/close status of transmission lines. The binary decision variable $U_{i,j}$ is defined to model the open/close status of candidate transmission line between nodes i and j. Due to network splitting, the admittance matrix of the system must be updated throughout the optimisation. According to (5)–(8), topological changes caused by the transmission switching (i.e. network splitting) are considered

$$BL_{i,j}^{new} = BL_{i,j}U_{i,j}, \quad i \neq j \tag{5}$$

$$BL_{i,i}^{new} = BL_{i,i} + \sum_{\substack{j=1 \\ j\neq i}}^{N_b} (1 - U_{i,j})BL_{i,j}, \quad i = j \tag{6}$$

$$GL_{i,j}^{new} = GL_{i,j}U_{i,j}, \quad i \neq j \tag{7}$$

$$GL_{i,i}^{new} = GL_{i,i} + \sum_{\substack{j=1 \\ j\neq i}}^{N_b} (1 - U_{i,j})GL_{i,j}, \quad i = j \tag{8}$$

The non-linear power balance constraints given in (3) and (4) are now linearised as follows:

$$\left[P_{gi}^0 + \Delta P_{l_i}^+ - \Delta P_{l_i}^- - P_{Li}\right] = \sum_{j=1}^{N_b} P_{ij}^{A1} \tag{9}$$

$$[Q_{Gi} - Q_{Li}] = \sum_{j=1}^{N_b} Q_{ij}^{A1} \tag{10}$$

where the Taylor expansion of the right-hand side of (9), around a small value of $(\theta_i - \theta_j)$ is obtained as follows:

$$P_{ij}^{A1} = (GL_{ij}(V_i + V_j - 1) + BL_{ij}(\theta_i - \theta_j))U_{ij}, \quad i \neq j \tag{11}$$

$$P_{ij}^{A1} = (2V_i - 1)GL_{ij} + \sum_{\substack{k=1 \\ k \neq i}}^{N_b} P_{ik}^{A2} GL_{ik}, \quad i = j \tag{12}$$

where

$$P_{ij}^{A2} = (2V_i - 1)\big(1 - U_{ij}\big) = (2V_i - 1) - P_{ij}^{A3}, \quad i \neq j \tag{13}$$

In (13), $P_{ij}^{A3} = (2V_i - 1)\big(U_{ij}\big)$. Now (11) is linearised as given by

$$\begin{aligned} -L(1 - U_{i,j}) \leq P_{ij}^{A1} - \big[GL_{ij}(V_i + V_j - 1) \\ + BL_{ij}\big(\theta_i - \theta_j\big)\big] \leq L(1 - U_{ij}), \quad i \neq j \end{aligned} \tag{14}$$

$$-LU_{i,j} \leq P_{ij}^{A1} \leq LU_{ij}, \quad i \neq j \tag{15}$$

Also, (13) is linearised as follows:

$$-LU_{i,j} \leq P_{ij}^{A2} - (2V_i - 1) \leq LU_{ij}, \quad i \neq j \tag{16}$$

$$-L\big(1 - U_{i,j}\big) \leq P_{ij}^{A2} \leq L\big(1 - U_{ij}\big), \quad i \neq j \tag{17}$$

In order to linearise Q_{ij}^{A1}, a similar procedure is done. The Taylor expansion of the right hand side of (10) is obtained as follows:

$$Q_{ij}^{A1} = \big[GL_{ij}\big(\theta_i - \theta_j\big) - BL_{ij}(V_i + V_j - 1)\big]U_{ij}, \quad i \neq j \tag{18}$$

$$Q_{ij}^{A1} = -\left[(2V_i - 1)BL_{ij} + \sum_{\substack{k=1 \\ k \neq i}}^{N_b} Q_{ik}^{A2} BL_{ik}\right], \quad i = j \tag{19}$$

where

$$Q_{ij}^{A2} = (2V_i - 1)\big(1 - U_{ij}\big) \tag{20}$$

Now (18) and (20) are linearised as given in (21)–(22) and (23)–(24), respectively

$$\begin{aligned} -L(1 - U_{ij}) \leq Q_{ij}^{A1} - [GL_{ij}\big(\theta_i - \theta_j\big) \\ - BL_{ij}(V_i + V_j - 1)] \leq L(1 - U_{ij}), \quad i \neq j \end{aligned} \tag{21}$$

$$-LU_{ij} \leq Q_{ij}^{A1} \leq LU_{ij}, \quad i \neq j \tag{22}$$

$$-LU_{ij} \leq Q_{ij}^{A2} - (2V_i - 1) \leq LU_{ij} \tag{23}$$

$$-L\big(1 - U_{i,j}\big) \leq Q_{ij}^{A2} \leq L\big(1 - U_{ij}\big) \tag{24}$$

- Operational constraints

The power flow limits across the transmission lines are considered using

$$-P_{ij}^{\max} \leq P_{ij} \leq P_{ij}^{\max}, \quad \forall ij \in \Omega^{1} \tag{25}$$

where

$$P_{ij} = P_{ij}^{A1} - P_{ij}^{A3} GL_{ij}, \quad i \neq j \tag{26}$$

The reactive power of generators and the voltage magnitudes of buses are constrained as given by

$$Q_{\mathrm{G}i}^{\min} \leq Q_{\mathrm{G}i} \leq Q_{\mathrm{G}i}^{\max}, \quad \forall i \in \Omega^{\mathrm{g}} \tag{27}$$

$$V_i^{\min} \leq V_i \leq V_i^{\max} \quad \forall i \in \Omega^{\mathrm{d}} \tag{28}$$

The constraints given in (3)–(28) describe the power balance constraints and the operational limits based on the linearised AC power flow equations. Instead of using DC power flow model, which is far from the real conditions of power system, in this paper the linearised AC power flow model is utilised to assure the power balance at each node, while preserving the technical limits on transmission lines, reactive power generations of generators and voltage limits. Also, a binary variable named U_{ij} is included in these constraints to update the network admittance matrix under splitting strategy.

- Connectivity and coherency constraints

According to the coherency constraint, all coherent generators must remain on the same island without any physical path between the non-coherent generators. The set of coherent groups of generators may be determined enough before the islanding execution using the slow coherency technique as proposed in [6]. In other words, the set of coherent generators is considered as the input of the MILP model. The connectivity of coherent generators and disconnectivity of non-coherent generators during the solution of the MILP model is satisfied by the impedance matrix. Two coherent generators i and j are in the same island if and only if the constraint (29) is satisfied. According to (29), when the ijth element of the impedance matrix is non-zero, it means that there is a physical path between two nodes i and j

$$Z_{ij} \neq 0 \quad \forall i \text{ and } j \in \Omega_{ns}^{\mathrm{g}} \tag{29}$$

The constraint given in (29) can be linearised as follows:

$$\frac{Z_{ij}}{L} < Su_{ij} < \frac{Z_{ij}}{L} + 1 \quad \forall i \text{ and } j \in \Omega_{ns}^{\mathrm{g}} \tag{30}$$

Based on (30), if $Z_{ij} = 0$ the binary variable Su_{ij} is restricted as $0 < Su_{ij} < 1$ (i.e. infeasible). Therefore, (30) enforces two coherent generators i and j to remain on the same island. Also, two non-coherent generators i and j are disconnected (i.e. are not in the same island) if and only if the constraint (31) is fulfilled

$$Z_{ij} = 0 \quad \forall i \in \Omega_{ns}^{\mathrm{g}} \text{ and } j \notin \Omega_{ns}^{\mathrm{g}} \tag{31}$$

4 Second stage: transient stability assessment

The transient stability of the controlled islanding scheme is fulfilled in this stage. In order to perfect the second stage of the proposed islanding scheme, two issues including the formulation of TEF and determination of saddle point or CUEP are introduced as follows.

4.1 Developing the TEF

In this paper, based on the rotor angles of synchronous generators, a TEF is developed to evaluate the transient stability of the splitting strategy found in the first stage. It is assumed that the values of rotor angles before and right after the controlled islanding execution are the same (i.e. no abrupt changes in rotor angles). In this regard, the developed TEF is evaluated individually for each resulted island based on the rotor angles measured by the PMUs. The proposed TEF needs just one sample of rotor angles before the controlled islanding. In order to introduce the proposed TEF, the swing equation of each synchronous machine in a system with n synchronous machines is supposed to be as follows [28]:

$$M_i\ddot{\delta}_i = P_{mi} - \frac{E_i^2}{Z_{ii}}\cos(\varnothing_{ii}) + \sum_{\substack{j=1 \\ i \neq j}}^{N_g} \frac{E_i E_j}{Z_{ij}}\cos\big(\delta_{ij} + \varnothing_{ij}\big) \tag{32}$$

Based on [28, 34], the relative swing equations for two synchronous machines are as follows:

$$
\begin{aligned}
&[M_j(M_i\ddot{\delta}_i) - M_i(M_j\ddot{\delta}_j)]\dot{\delta}_{ij} = M_iM_j\ddot{\delta}_{ij}\dot{\delta}_{ij} \\
&= M_j\left[P_{mi} - \frac{E_i^2}{Z_{ii}}\cos(\varnothing_{ii}) + \sum_{j=1}^{N_g}\frac{E_iE_j}{Z_{ij}}\cos\left(\delta_{ij} + \varnothing_{ij}\right)\right]\dot{\delta}_{ij} \\
&-M_i\left[P_{mj} - \frac{E_j^2}{Z_{jj}}\cos\left(\varnothing_{jj}\right) + \sum_{i=1}^{N_g}\frac{E_jE_i}{Z_{ji}}\cos\left(\delta_{ji} + \varnothing_{ji}\right)\right]\dot{\delta}_{ij}
\end{aligned} \tag{33}
$$

To reach a TEF, and for the sake of simplicity, the relative swing equations for a system with three synchronous machines are extracted as follows:

$$
\begin{cases}
M_1M_2\ddot{\delta}_{12}\dot{\delta}_{12} + M_1M_3\ddot{\delta}_{13}\dot{\delta}_{13} + M_2M_3\ddot{\delta}_{23}\dot{\delta}_{23} \\
= +M_3\dfrac{E_1E_2}{Z_{12}}\left[\cos(\delta_{12} + \varnothing_{12})\dot{\delta}_{13} - \cos(\delta_{12} - \varnothing_{12})\dot{\delta}_{23}\right] \\
+M_2\dfrac{E_1E_3}{Z_{13}}\left[\cos(\delta_{13} + \varnothing_{13})\dot{\delta}_{12} + \cos(\delta_{13} - \varnothing_{13})\dot{\delta}_{23}\right] \\
+M_1\dfrac{E_2E_3}{Z_{23}}\left[\cos(\delta_{23} - \varnothing_{23})\dot{\delta}_{13} - \cos(\theta_{23} + \varnothing_{23})\dot{\delta}_{12}\right] \\
+\left[M_2\dfrac{E_1E_2}{Z_{12}}\cos(\delta_{12} + \varnothing_{12}) + M_1\dfrac{E_1E_2}{Z_{12}}\cos(\delta_{12} - \varnothing_{12})\right]\dot{\delta}_{12} \\
+\left[M_3\dfrac{E_2E_3}{Z_{23}}\cos(\delta_{23} + \varnothing_{23}) + M_2\dfrac{E_2E_3}{Z_{23}}\cos(\delta_{23} - \varnothing_{23})\right]\dot{\delta}_{23} \\
+\left[M_3\dfrac{E_1E_3}{Z_{13}}\cos(\delta_{13} + \varnothing_{13}) + M_1\dfrac{E_1E_3}{Z_{13}}\cos(\delta_{13} - \varnothing_{13})\right]\dot{\delta}_{13} \\
+\left\{M_2\left[P_{m1} - \dfrac{E_1^2}{Z_{11}}\cos(\varnothing_{11})\right] - M_1\left[P_{m2} - \dfrac{E_2^2}{Z_{22}}\cos(\varnothing_{22})\right]\right\}\dot{\delta}_{12} \\
+\left\{M_3\left[P_{m1} - \dfrac{E_1^2}{Z_{11}}\cos(\varnothing_{11})\right] - M_1\left[P_{m3} - \dfrac{E_3^2}{Z_{33}}\cos(\varnothing_{33})\right]\right\}\dot{\delta}_{13} \\
+\left\{M_3\left[P_{m2} - \dfrac{E_2^2}{Z_{22}}\cos(\varnothing_{22})\right] - M_2\left[P_{m3} - \dfrac{E_3^2}{Z_{33}}\cos(\varnothing_{33})\right]\right\}\dot{\delta}_{23}
\end{cases} \tag{34}
$$

To derive a suitable TEF it is required to integrate (34), over the interval $\left[\delta^s, \delta^R\right]$ (i.e. from saddle-point to real time rotor angle). However, the first three terms located in the right hand side of (34) cannot be integrated due to the existence of dependent variables in each term (e.g. δ_{12} and $\dot{\delta}_{13}$ in $\cos(\delta_{12} + \varnothing_{12})\dot{\delta}_{13}$). Assuming a lossless network, each of the first three terms may be rewritten as follows:

$$
M_3\frac{E_1E_2}{Z_{12}}\sin(\delta_{12})\left[-\dot{\delta}_{13} + \dot{\delta}_{23}\right] = M_3\frac{E_1E_2}{Z_{12}}\sin(\delta_{12})[-\dot{\delta}_{12}] \tag{35}
$$

Therefore, the indefinite integral of (34) is obtained as follows:

$$
\begin{aligned}
&\frac{M_1M_2\ddot{\delta}_{12}^2}{2} + \frac{M_1M_3\ddot{\delta}_{13}^2}{2} + \frac{M_2M_3\ddot{\delta}_{23}^2}{2} \\
&= [M_2 + M_1 + M_3]\left\{\frac{E_1E_2}{Z_{12}}\cos(\delta_{12}) + \frac{E_2E_3}{Z_{23}}\cos(\delta_{23})\right. \\
&\left.+\frac{E_1E_3}{Z_{13}}\cos(\delta_{13})\right\}T_{m_{12}}(\delta_{12}) + T_{m_{13}}(\delta_{23}) + T_{m_{23}}(\delta_{13})
\end{aligned} \tag{36}
$$

where

$$
T_{m_{ij}} = M_j[P_{mi}] - M_i[P_{mj}] \tag{37}
$$

Now, to extend the TEF formulation to a n-machine system, the expression given in (36) is integrated over the interval of $[\delta_s, \delta_R]$ as follows:

$$
\begin{aligned}
&\frac{1}{\sum_{i=1}^{N_g}M_i}\sum_{i=1}^{N_g-1}\sum_{j=i+1}^{N_g}\frac{M_iM_j\omega_{ij}^{R^2}}{2} = \sum_{i=1}^{N_g-1}\sum_{j=i+1}^{N_g}\frac{E_iE_j}{Z_{ij}}[\cos\left(\delta_{ij}^{\mathrm{R}}\right) \\
&-\cos\left(\delta_{ij}^{\mathrm{s}}\right)] + \sum_{i=1}^{N_g-1}\sum_{j=i+1}^{N_g}P_{m_{ij}}\left(\delta_{ij}^{\mathrm{R}} - \delta_{ij}^{s}\right)
\end{aligned} \tag{38}
$$

It is noted that $\ddot{\delta}_{ij}$ at saddle point is zero. According to (38), the general formulation of the potential and kinetic energy for a system consisting of n-machines are determined as follows:

$$
\begin{aligned}
&En_p = \sum_{i=1}^{N_g-1}\sum_{j=i+1}^{N_g}\frac{E_iE_j}{Z_{ij}}[\cos\left(\delta_{ij}^{\mathrm{R}}\right) - \cos\left(\delta_{ij}^{s}\right)] + \sum_{i=1}^{N_g-1}\sum_{j=i+1}^{N_g} \\
&T_{m_{ij}}\left(\delta_{ij}^{\mathrm{R}} - \delta_{ij}^{s}\right)
\end{aligned} \tag{39}
$$

$$
En_k = \frac{1}{\sum_{i=1}^{N_g}M_i}\sum_{i=1}^{N_g-1}\sum_{j=i+1}^{N_g}\frac{M_iM_j\omega_{Rij}^2}{2} \tag{40}
$$

The transient stability is preserved if $En_k - En_p < 0$ [34]. Indeed, this criterion is calculated for each island based on the mechanical power and δ_{ij}^{R} (i.e. relative rotor angle).

4.2 Finding the control UEP or saddle point

To evaluate the transient stability of a given controlled islanding strategy using the proposed TEF, the saddle or CUEP (i.e. δ_{ij}^s) must be determined. Different methods have been developed for determining the control UEP [28, 34]. In this section, two different methods have been proposed to calculate CUEPs.

- Method 1

  In the second stage, a saddle point is determined using a non-linear programming (NLP) optimisation problem. At a given saddle point, the following issues are considered:
- a At the saddle point, the following condition must be fulfilled (i.e. in saddle point $\ddot{\delta}_{ij} = 0$):

$$
\begin{aligned}
&M_j\left[P_{mi} - \frac{E_i^2}{Z_{ii}}\cos(\varnothing_{ii}) + \sum_{j=1}^{N_g}\frac{E_iE_j}{Z_{ij}}\cos\left(\delta_{ij} + \varnothing_{ij}\right)\right] \\
&-M_i\left[P_{mj} - \frac{E_j^2}{Z_{jj}}\cos\left(\varnothing_{jj}\right) + \sum_{i=1}^{N_g}\frac{E_jE_i}{Z_{ji}}\cos\left(\delta_{ji} + \varnothing_{ji}\right)\right] = 0
\end{aligned} \tag{41}
$$

- b According to the mutual torque between two given generators, i and j given in (37), for small positive values of $T_{m_{ij}}$ the saddle point (i.e. δ_{ij}^s) should be selected as close to 180° as possible and for the negative values of $T_{m_{ij}}$ the saddle point is selected close to zero [28, 34]. These conditions are formulated as a simple NLP optimisation model via the objective function given in (42) and the constraint expressed by (43)

$$
\mathrm{SD} = \min\sum_{i=1}^{N_g-1}\sum_{j=i+1}^{N_g}\left(\delta_i - \delta_j - \pi\, Bu_{ij}\right)^2 \tag{42}
$$

$$
\ddot{\delta}_{ij} = 0 \tag{43}
$$

  where the binary parameter Bu_{ij} is determined as follows:

$$
\begin{cases}
Bu_{ij} = 0 & \text{if } -\gamma \le T_{m_{ij}} \le \gamma \\
Bu_{ij} = 1 & \text{if } T_{m_{ij}} \left\langle -\gamma \text{ or } T_{m_{ij}} \right\rangle \gamma
\end{cases} \tag{44}
$$

  The optimisation model (42)–(44) is solved separately for each island. It is noted that this simple NLP model is not included in the MILP model of the first stage. According to (42)–(44), when absolute value of $T_{m_{ij}}$ is greater than γ, Bu_{ij} will be equal to 1 and the saddle point is selected close to 180, otherwise the saddle point is selected close to zero.
- Method 2

The following steps are taken to estimate the saddle point of the power system at an operating condition [28]:

Step 1. Find the SEP (i.e. δ_{ij}^{sep}) using the steady-state power flow model.

Step 2. Find the set of equilibrium points (i.e. δ_{ij}^{eq}) using (43).

Step 3. Identify those equilibrium points whose unstable manifolds contain trajectories approaching the SEP obtained in step 1.

All three steps could be done by minimising (45) subject to (43)

$$\min\left\{E_p\left(E,\delta_{ij}^{\text{sep}}\right)-E_p\left(E,\delta_{ij}^{\text{s}}\right)\right\} \tag{45}$$

The aim of the objective function given in (45) is to minimise the difference between the potential energy at δ_{ij}^{sep} and δ_{ij}^{s}. The potential energy is calculated using (39). Majority of procedures proposed for determining UEPs have some degree of approximation. Due to this approximation, it is possible to identify non-controlling UEP as controlling UEP.

5 Constructing linear constraint

In the second stage using the proposed TEF, the transient stability of the splitting strategy is evaluated. When the transient stability is met, the obtained solution is the final strategy, otherwise, a new constraint must be constructed to update the current splitting strategy. To this end, a sensitivity-based approach is introduced to update the transfer impedance between pairs of generators with more impact on TEF-based stability criterion. Indeed by changing the splitting strategy, the potential energy of each island as well as TEF-based stability criterion is changed. In the second stage, the parameter $S_{i,j}$ is calculated as follows:

$$S_{ij}^{(k)}=\left|\frac{E_iE_j}{Z_{ij}}[\cos\left(\delta_{i,j}^{\text{R}}\right)-\cos\left(\delta_{ij}^{\text{s}}\right)]\times\left[Z_{ij}^{c}-Z_{ij}^{is(k)}\right]\right| \tag{46}$$

Assume that the transfer impedance between two generators l and m is expressed as follows:

$$Z_{lm}^{(k+1)}=Z_{lm}^{(k)}\pm\Delta Z_{lm}^{(k)}\simeq\alpha_{lm}^{(k)}Z_{lm}^{(k)} \tag{47}$$

where $\alpha_{lm}^{(k)}$ is a limiting factor. According to (46), the generator pair (l,m) with the highest value of $S_{i,j}$ in each unstable island is selected to construct a linear constraint to be added to the MILP model of the first stage. The sensitivity values are calculated for the generators of each island separately. No optimisation model is needed to calculate the sensitivity analysis. Also, the term of $\left[Z_{ij}^{c}-Z_{ij}^{is(k)}\right]$ is considered in (46) to select the pair of (l,m) with higher sensitivity to the islanding boundary change.

In order to meet the stability criterion (i.e. $En_k-En_p<0$) it is needed to increase the amount of potential energy during the iterative process between the first and second stages. By changing the impedance Z_{lm} (i.e. by the splitting strategy) the location of saddle point and the amount of potential energy in each resulted island are changed. It is noted that according to (40), the kinetic energy is not changed by line splitting at instant of islanding. Indeed, to construct the linear constraint, the variation of potential energy and the saddle point caused by the change of $Z_{l,m}$ are approximated. To fulfil the first condition of saddle point given in (41), the following relation must be satisfied in two subsequent iterations between the first and second stages:

$$\frac{E_lE_m}{\alpha_{lm}^{(k)}Z_{lm}^{(k)}}\sin\left(\delta_{lm}^{s\,(k+1)}\right)\simeq\frac{E_lE_m}{Z_{lm}^{(k)}}\sin\left(\delta_{lm}^{s\,(k)}\right) \tag{48}$$

Assuming constant values of E_l and E_m, the constraint given in (48) is simplified as follows:

$$\sin\left(\delta_{lm}^{s\,(k+1)}\right)\simeq\alpha_{lm}^{(k)}\sin\left(\delta_{lm}^{s\,(k)}\right) \tag{49}$$

According to the second condition of the saddle point given in (42)–(44), the following approximations are valid:

$$\delta_{lm}^{s\,(k+1)}\simeq\alpha_{lm}^{(k)}\delta_{lm}^{s\,(k)}\quad\text{if }\delta_{lm}^{s\,(k)}\simeq0 \tag{50}$$

$$\delta_{lm}^{s\,(k+1)}-\pi\simeq\alpha_{lm}^{(k)}\left(\delta_{lm}^{s\,(k)}-\pi\right)\quad\text{if }\delta_{lm}^{s\,(k)}\simeq\pi \tag{51}$$

The variation of potential energy due to the change of $Z_{l,m}$ and saddle point is now determined using the following equation:

$$\begin{aligned}\Delta En_P\simeq{}&\frac{E_lE_m}{\alpha_{lm}^{(k)}Z_{lm}^{(k)}}[\cos\left(\delta_{lm}^{R}\right)-\cos\left(\delta_{lm}^{s\,(k+1)}\right)]-\frac{E_lE_m}{Z_{lm}^{(k)}}\\&\times\ [\cos\left(\delta_{lm}^{R}\right)-\cos\left(\delta_{lm}^{s\,(k)}\right)]-P_{m_{l,m}}\left(\delta_{lm}^{s\,(k+1)}\right)P_{m_{ij}}\left(\delta_{lm}^{s\,(k)}\right),\end{aligned} \tag{52}$$

According to (42)–(44) and (50), if $\delta_{lm}^{s\,(k)}\simeq0$ then (52) is expressed as follows:

$$\Delta En_P=\frac{E_lE_m}{Z_{lm}^{(k)}}[\cos\left(\delta_{lm}^{R}\right)-1]\left[\frac{1}{\alpha_{lm}^{(k)}}-1\right] \tag{53}$$

Based on the stability criterion (i.e. $E_K-E_P\le0$), to satisfy the transient stability constraint, the variation of potential energy must be positive (i.e. $\Delta En_P>0$) during the iterative process. To this end, the limiting factor of $\alpha_{lm}^{(k)}$ must be selected >1. According to (42)–(44) and (51), if $\delta_{lm}^{s\,(k)}\simeq\pi$, then (52) is expressed as follows:

$$\Delta En_P=\frac{E_lE_m}{Z_{lm}^{(k)}}[\cos\left(\delta_{lm}^{\text{R}}\right)+1]\left[\frac{1}{\alpha_{lm}^{(k)}}-1\right] \tag{54}$$

In this case, to have a positive variation of potential energy (i.e. $\Delta E_P>0$), the limiting factor of $\alpha_{lm}^{(k)}$ must be selected lower than 1.

Based on (53)–(54) if $\delta_{lm}^{s\,(k)}\simeq\pi$, the constraint (55) and if $\delta_{lm}^{s\,(k)}\simeq0$ the constraint (56) is used as the linear constraint in MILP model

$$Z_{lm}^{(k+1)}\le\alpha_{lm}^{(k)}Z_{lm}^{(k)} \tag{55}$$

$$Z_{lm}^{(k+1)}\ge\alpha_{lm}^{(k)}Z_{lm}^{(k)} \tag{56}$$

6 Calculation of impedance matrix in the MILP model

As the constraints (29)–(31) and (55)–(56) were formulated as a function of transfer impedance, hence to include the linear constraint in the MILP model, it is required to compute the electrical impedance between the generators of each island efficiently. The relation between the impedance and admittance matrices is defined as follows:

$$I=Z\cdot Y \tag{57}$$

The basic relation given in (57) results in N non-linear equations. This constraint is linearised and calculated only for generator buses. In a lossless system, assume (g,j) element of the vector equation given in (58), as follows:

$$I_g(g,j)=\sum_{i=1}^{N_b}Z_{gi}\times BL_{ij}^{new} \tag{58}$$

Using the auxiliary variable of $D_{gij}=Z_{gi}\times BL_{ij}^{\text{new}}$ and according to (5)–(8), the constraints given in (59)–(64) are the linear equivalents of (58)

$$I_g(g,j) = \sum_{i=1}^{N_b} D_{gij} \tag{59}$$

$$-L(1-U_{ij}) \le D_{gij} - Z_{gi}BL_{ij} \le L(1-U_{ij}), \quad j \ne i \tag{60}$$

$$-LU_{ij} \le D_{gij} \le LU_{ij}, \quad j \ne i \tag{61}$$

$$D_{gii} = Z_{gi} \times BL_{ii} + \sum_{j=1, j\ne i}^{N_b} D^A_{gij} \tag{62}$$

$$-LU_{ij} \le D^A_{gij} - Z_{gi}BL_{ij} \le LU_{ij}, \quad j \ne i \tag{63}$$

$$-L(1-U_{ij}) \le D^A_{gij} \le L(1-U_{ij}), \quad j \ne i \tag{64}$$

7 Simulation results

The proposed transient stability constrained controlled islanding model is implemented in dynamic IEEE 118-bus test system [35]. The required transient stability simulations have been done in DIgSILENT transient stability simulator. All the optimisation models including the MILP model of controlled islanding in the first stage are solved using CPLEX in GAMS. Also, the optimisation model developed for determining saddle points in the second stage is solved by SBB in GAMS using a PC with Intel core i7, 4.2 GHz 7700 CPU, and 32 GB DDR4 RAM. Two different cases are simulated. In the first case, the MIP-only model proposed for controlled islanding problem is simulated without considering the transient stability criterion (i.e. first iteration of the proposed algorithm). In the second case, the efficacy of the proposed transient stability constrained controlled islanding model (i.e. the iterative two-stage algorithm) is investigated. For both cases, it is assumed that a delayed three-phase short circuit fault is occurred at $t = 0.2$ s at node 77 and is cleared at $t = 0.4$ s. According to Fig. 2, without any remedial action the synchronous machine located at node 80 goes out of step at $t = 1.8$ s. After tripping G80, the generators G89, G100, G103 and G111 will trip in 3 s due to pole slipping or out-of-step condition. Finally, without any remedial action the entire grid faces a complete blackout and the total load of network (i.e. 3668 MW) is lost. Two conventional and transient stability constrained islanding strategies are utilised to stop the propagation of the cascading failure as follows.

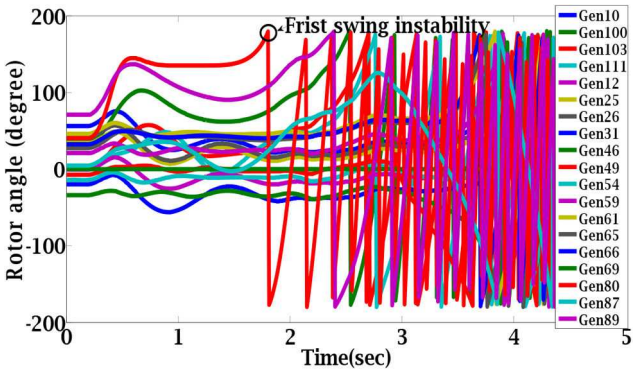

Fig. 2 *Trajectories of rotor angles without any remedial actions*

7.1 Case A: MILP-only based controlled islanding

The MILP formulation of controlled islanding is solved and the obtained strategy is then executed. The optimal splitting strategy has been reported in Table 1 (i.e. iteration 1 of the iterative process). The total simulation time of optimisation is 0.01 s which make it suitable to be implemented as a near real-time action. The obtained strategy is now applied to the network to verify its inefficacy in providing transient stability. According to Fig. 3, it can be seen that due to ignoring the transient stability in MILP model, the second island is not stable and the G80 and a little later other generators face the transient instability. Indeed, the strategy obtained by MILP-only islanding is considered as the initial solution of the iterative controlled islanding and hence the inefficacy of this solution in transient stability's point of view is investigated more in next simulation case.

7.2 Case B: transient stability constrained controlled islanding

In this case, the iterative two-stage controlled islanding scheme is simulated. The results of the first stage (i.e. conventional islanding) are reported in Table 1. This solution is sent to the second stage to be evaluated in transient stability's point of view. As discussed before, using MILP-only strategy the second island does not fulfil the transient stability criterion. According to Table 1, it can be seen that the transient stability criterion is as $En_k - En_p = 2.561 > 0$ which confirm the instability of the obtained splitting strategy in the second island. In the second iteration, the most important generators in each island are identified based on the sensitivity analysis proposed in (46). The impedance between these sensitive

Table 1 Result of proposed two-stage algorithm in each iteration

Iteration (CPU time)	Splitting lines	Island no.	$E_K - E_P$	Stability check		Total imbalance	Selected Z_{ij}/S_{ij}	$Z^c_{ij} - Z^{is(k)}_{ij}$	$\delta^{s(k)}_{lm}$	$\alpha^{(k)}_{lm}$
				TEF	Full simulation					
1 (0.01 s)	19–34, 24–72, 30–38, 33–37, 24–70, 77–82, 80–98, 80–97, 80–96, 99–100	1	12.60–13.32	✓	✓	154 MW	—	—	—	—
		2	3.21–0.65	⊗	⊗		(69, 80)/9.75	0.041–0.145	131	0.98
		3	0.17–27.98	✓	✓		—	—	—	—
2 (0.03 s)	33–37, 19–34, 24–72, 30–38, 24, 70, 77–82, 80–97, 80–96, 98–100, 99–100	1	12.60–12.76	✓	✓	218 MW	—	—	—	—
		2	3.21–1.29	⊗	⊗		(69, 80)/9.68	0.041–0.141	132.2	0.98
		3	0.17–27.68	✓	✓		—	—	—	—
3 (0.02 s)	33–37, 19–34, 23–24, 30–38, 77–82, 80–97, 80–96, 98–100, 99–100	1	12.60–12.76	✓	✓	220 MW	—	—	—	—
		2	3.21–2.811	⊗	✓		(46, 65)/9.51	0.052–0.151	131.7	0.98
		3	0.17–25.13	✓	✓		—	—	—	—
4 (0.01 s)	15–33, 19–34, 23–24, 30–38, 77–82, 80–97, 80–96, 98–100, 99–100	1	12.60–12.76	✓	✓	259.8 MW	—	—	—	—
		2	3.21–3.62	✓	✓		—	—	—	—
		3	0.17–23.95	✓	✓		—	—	—	—

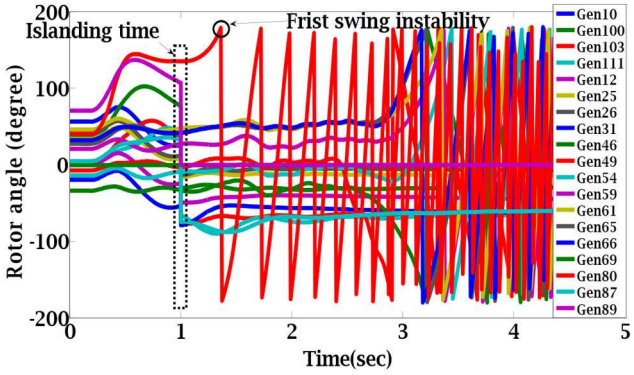

Fig. 3 *Trajectories of rotor angles under the conventional controlled islanding*

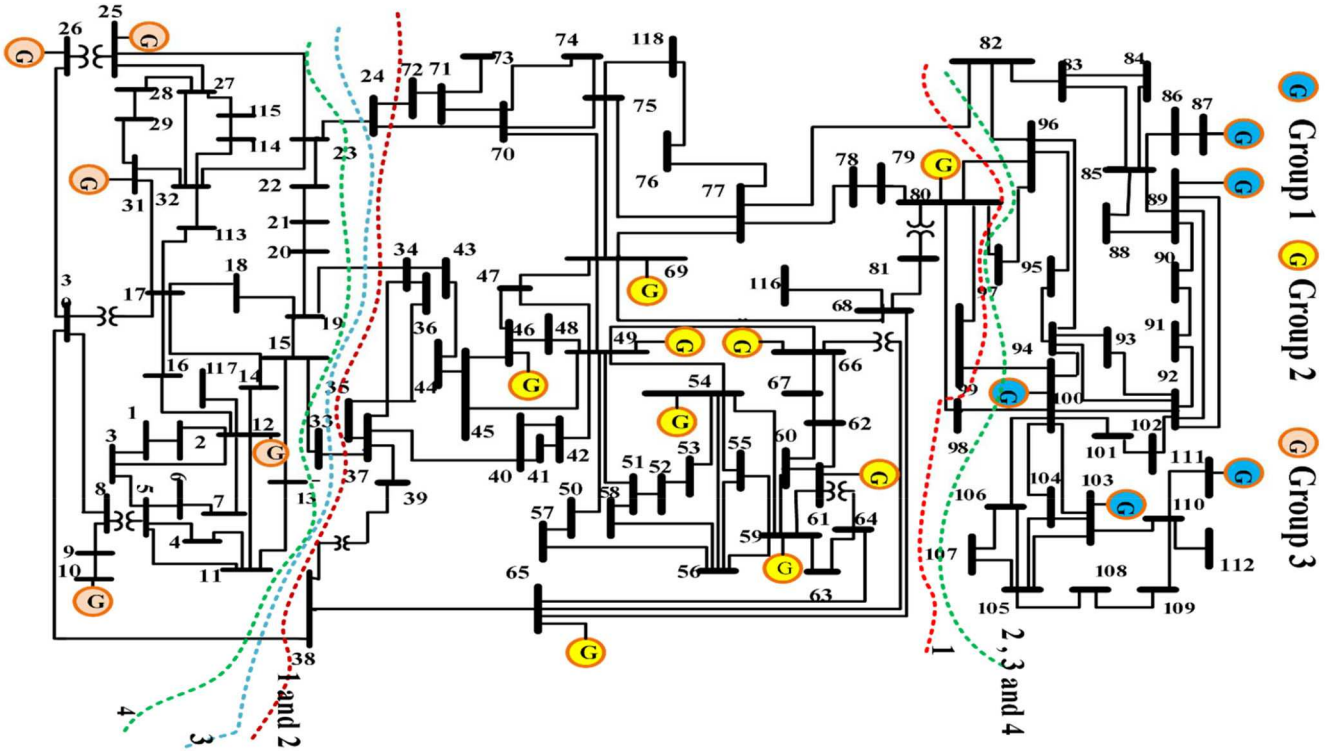

Fig. 4 *Island boundaries in four iterations of the proposed model*

generators is then utilised to construct the linear constraint according to (55)–(56). According to (46), the generator pair of (G69, G80) is selected from the second island (i.e. unstable island).

The impedance between this pair of generators is then selected to construct the linear constraint to be added to the MILP model of the first stage (i.e. second iteration). The limiting factor is selected to adjust the impedance between the generator pairs of (G69, G80) to satisfy the transient stability criterion. To this end, the amount of limiting factor at the first iteration is set as i.e. $\alpha^{(1)}_{69,80} = 0.98$. It is noted that the normal or default value of limiting factor is 1 (i.e. $\alpha^{(0)}_{69,80} = 1$). By assigning a limiting factor very close to 1, the risk of slow convergence is expected. Also by assigning a limit factor far from 1, the risk of divergence is increased. According to Table 1, this iterative process is converged at the fourth iteration. As shown in the first column of Table 1, the total CPU time of the proposed method is 0.07 s which makes the proposed method promising for online applications. In the fifth column of Table 1, the results of stability check using the energy-based criterion and the full numerical transient simulation using DIgSILENT have been compared. It can be seen that at the third iteration the full numerical simulations confirm the stability of the obtained strategy, however, the energy-based criterion will not confirm the stability. At the fourth iteration, both the energy-based criterion and the full scale numerical simulations confirm the transient stability. In this case, it can be concluded that the energy-based criterion is a little conservative rather than the actual numerical simulations with 39.8 MW additional load shedding. Although the proposed method results in more shed in this test case, however using the proposed TEF method, the full time-consuming simulation is avoided. Unlike the TEF-based islanding method, the full numerical transient stability simulation is not able to govern the MIP model to select the proper splitting lines to improve the transient stability of unstable islands. The changes in islanding boundaries in each iteration are shown in Fig. 4. As shown in Fig. 4, the change of islanding boundary in each iteration is very informative (i.e. the islanding boundaries of two consecutive iterations are close together). The trajectories of rotor angles under the splitting strategy obtained at the fourth iteration have been illustrated in Fig. 5. According to Fig. 6, it can be seen that during the iterative procedure, the potential energy of each island is changed. The amount of potential energy in each island is evolved such that the potential energy in each island is greater than the kinetic energy of that island and hence the stability criterion is fulfilled. Also, the variation of saddle points during the iterative process has been reported in Table 2. The value of saddle points using Method-1 and Method-2 is reported in Table 2. As given in Table 2, both methods give approximately similar estimation of saddle point or CUEP. It can be seen that the maximum variation of the saddle point is related to the pair of (G69, G80) in iterations 2 and 3 and the pair of (G46, G65) in iteration 4. Also, the CUEP using both methods are reported in Table 3 for the interconnected system without

executing any controlled islanding plan. The point in which the systems experience the out-of-step conditions is reported in Table 3. The potential energy difference between each of these points and the SEP is reported at the end of Table 3. It can be seen that the CUEPs obtained using methods 1 and 2 give lower potential energy.

Unlike the closest UEP, the controlling UEP method takes into account the fault-on trajectory. It is evident that the critical energy value obtained using the controlling UEP method is greater than the critical energy value calculated by the closest UEP method [28]. Therefore, the controlling UEP method does not suffer from the excessively conservative essence of the closest UEP method. To this end, in this paper, the direct transient stability assessment was carried out using the controlling UEP method. According to [28], the only situation that the controlling UEP method gives a conservative stability assessment is the following: when the fault is cleared after the fault-on trajectory hits the constant energy surface passing through the controlling UEP and before it reaches the exit point. In such condition, the controlling UEP method classifies a stable contingency as unstable. Transient stability analysis is the study of whether the post-fault trajectory will converge to an acceptable equilibrium point. In order to assess the transient stability using the controlling UEP, it is required to show if fault-on trajectory at fault clearing time is lying inside the stability region of a desired stable UEP. The problem of computing controlling UEPs is expressed as a non-linearly constrained optimisation problem. In order to reach the true controlling UEPs, it is required to consider accurate system models in the non-linear optimisation problem.

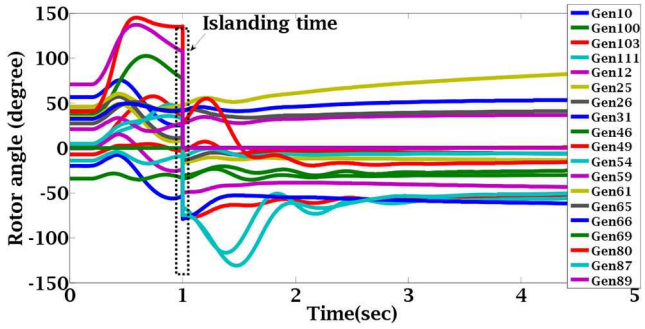

Fig. 5 *Trajectories of rotor angles under the proposed controlled islanding*

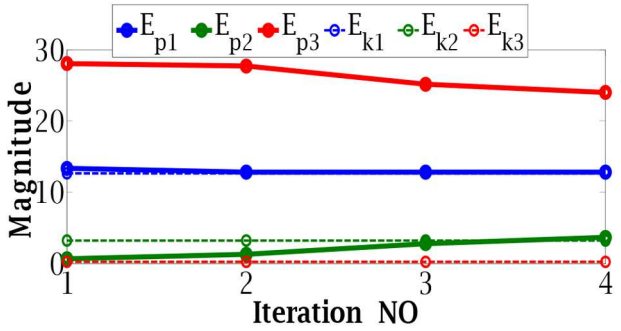

Fig. 6 *Changes of potential energy in each iteration of the proposed algorithm*

8 Conclusion

In this paper, a two-stage algorithm was proposed to consider the transient stability in controlled islanding plan. The major findings of this paper are summarised as follows: (i) the obtained results confirmed that without considering the transient stability constraints the splitting strategy obtained from the MIP-only controlled islanding model may fail to stabilise the resulted islands, (ii) the proposed TEF-based MIP islanding method preserves the transient stability of resulted islands by selecting the proper splitting lines. It was shown that the transient stability assessment by the proposed islanding method is comparable with the full dynamic simulation using a transient stability simulator, (iii) the proposed islanding method will converge in a few iterations between the first and second stages, with reasonable CPU times. The constructed linear constraint preserves the transient stability of created islands by adjusting the potential energy of each island and (iv) although the energy-based criterion results in a little conservative plan with small additional load shedding, the full time-consuming simulation is avoided using the proposed method. Unlike the TEF-based islanding method, the full numerical transient stability simulation is not able to govern the MIP model to select the proper splitting lines to improve the transient stability of unstable islands. Majority of procedures proposed for determining UEPs have some degree of approximation. Due to this approximation, it is possible to identify non-controlling UEP as controlling UEP. To remove this problem, accurate optimisation problem can be defined for determining true controlling UEPS. In this paper, it was assumed that the rotor angles of synchronous

Table 2 Saddle points (CUEP) in each iteration of the proposed algorithm

Group	Gen No.	CUEP or saddle point							
		Iteration 1		Iteration 2		Iteration 3		Iteration 4	
		Method 1	Method 2	Method 1	Method 2	Method 1	Method 2	Method 1	Method 2
1	10	180	191.80	180	181.53	180	193.51	180	199.23
	12	161.80	162.37	161.40	157.33	160.18	178.05	160.28	175.81
	25	0	0	0	0	0.83	0.61	0.91	0.95
	26	163.20	178.44	163.89	159.20	167.07	181.29	167.07	181.05
	31	153.60	164.02	153.11	153.69	156.23	177.02	156.23	166.57
2	46	24.18	26.01	24.58	24.66	24.39	27.03	22.88	25.841
	49	35.18	37.79	35.32	36.55	35.12	38.80	34.96	37.79
	54	38.23	39.72	38.07	39.98	38.41	43.85	38.10	42.018
	59	31.36	33.41	31.23	31.508	30.04	32.40	28.96	30.88
	61	34.25	34.83	33.89	33.01	33.01	37.16	32.62	36.21
	65	158.53	169.72	158.18	152.97	156.13	160.70	156.24	168.16
	66	34.49	34.59	34.26	33.65	33.91	36.89	33.15	36.97
	69	150.53	152.09	151.12	154.65	152.31	168.57	143.12	160.14
	80	19.56	20.655	18.94	21.079	17.18	18.16	16.41	18.45
3	87	19.82	20.01	19.82	20.44	20.45	21.58	20.91	22.89
	89	105.93	114.65	105.93	103.21	108.17	119.32	113.17	119.77
	100	14.73	15.75	14.81	15.36	15.36	17.32	16.33	17.52
	103	24.22	24.98	24.11	23.85	24.27	27.75	24.14	27.55
	111	180	197	180	174.53	180	191.33	179.1	190.78

Table 3 Saddle points (CUEP) for non- islanded system

Group	Gen No.	CUEP or saddle point		
		Method 1	Method 2	Out of step point
1	10	146.65	150.25	22.254
	12	146.55	151.14	19.73
	25	0	0	11.12
	26	149.06	157.87	15.60
	31	97.130	101.39	−40.06
2	46	2.35	2.59	35.39
	49	9.79	10.50	−2.852
	54	20.90	22.33	−11.26
	59	30.02	33.46	24.41
	61	33.04	34.22	46.18
	65	24.98	27.34	37.76
	66	33.47	36.62	40.40
	69	144.08	150.93	0
	80	9.49	10.16	176.92
3	87	15.86	16.01	25.02
	89	15.03	15.13	108.65
	100	6.21	6.62	75.92
	103	22.17	24.32	33.27
	111	142.59	159.23	35.48
$E_p(E,\delta_{ij}^s) - E_p(E,\delta_{ij}^{sep})$		12.154	13.871	26.364

machine are required to be gathered by a WAMS. However, in practice, all these data are not available or some data are missing. Also, the data transmission to the control centre comes up with time delay. Implementation of a transient stability constrained islanding method with limited amount of wide area measurement and the impact of delay in data transmission are open question that can be addressed in future works.

9 References

[1] Senroy, N., Heydt, G.T.: 'A conceptual framework for the controlled islanding of interconnected power systems', *IEEE Trans. Power Syst.*, 2006, **21**, (2), pp. 1005–1006

[2] Xu, G., Vittal, V., Meklin, A., *et al.*: 'Controlled islanding demonstrations on the WECC system', *IEEE Trans. Power Syst.*, 2010, **26**, (1), pp. 334–343

[3] Esmaeilian, A., Kezunovic, M.: 'Prevention of power grid blackouts using intentional islanding scheme', *IEEE Trans. Ind. Appl.*, 2016, **53**, (1), pp. 622–629

[4] Senroy, N., Heydt, G.T., Vittal, V.: 'Decision tree assisted controlled islanding', *IEEE Trans. Power Syst.*, 2006, **21**, (4), pp. 1790–1797

[5] Kundur, P., Paserba, J., Vitet, S.: 'Overview on definition and classification of power system stability'. CIGRE/IEEE PES Int. Symp. Quality and Security of Electric Power Delivery Systems, 2003. CIGRE/PES 2003, Montreal, Quebec, Canada, 2003, pp. 1–4

[6] You, H., Vittal, V., Wang, X.: 'Slow coherency-based islanding', *IEEE Trans. Power Syst.*, 2004, **19**, (1), pp. 483–491

[7] Vittal, V., Kliemann, W., Ni, Y.-X., *et al.*: 'Determination of generator groupings for an islanding scheme in the Manitoba hydro system using the method of normal forms', *IEEE Trans. Power Syst.*, 1998, **13**, (4), pp. 1345–1351

[8] Barocio, E., Korba, P., Sattinger, W., *et al.*: 'Online coherency identification and stability condition for large interconnected power systems using an unsupervised data mining technique', *IET Gener. Transm. Distrib.*, 2019, **13**, (15), pp. 3323–3333

[9] Babaei, M., Muyeen, S., Islam, S.: 'Identification of coherent generators by support vector clustering with an embedding strategy', *IEEE Access*, 2019, **7**, pp. 105420–105431

[10] Aghamohammadi, M., Tabandeh, S.: 'A new approach for online coherency identification in power systems based on correlation characteristics of generators rotor oscillations', *Int. J. Electr. Power Energy Syst.*, 2016, **83**, pp. 470–484

[11] Yusof, S., Rogers, G., Alden, R.: 'Slow coherency based network partitioning including load buses', *IEEE Trans. Power Syst.*, 1993, **8**, (3), pp. 1375–1382

[12] Yang, B., Vittal, V., Heydt, G.T.: 'Slow-coherency-based controlled islanding – a demonstration of the approach on the August 14, 2003 blackout scenario', *IEEE Trans. Power Syst.*, 2006, **21**, (4), pp. 1840–1847

[13] Xu, G., Vittal, V.: 'Slow coherency based cutset determination algorithm for large power systems', *IEEE Trans. Power Syst.*, 2009, **25**, (2), pp. 877–884

[14] Kyriacou, A., Demetriou, P., Panayiotou, C., *et al.*: 'Controlled islanding solution for large-scale power systems', *IEEE Trans. Power Syst.*, 2017, **33**, (2), pp. 1591–1602

[15] Quirós-Tortós, J., Demetriou, P., Panteli, M., *et al.*: 'Intentional controlled islanding and risk assessment: a unified framework', *IEEE Syst. J.*, 2017, **12**, (4), pp. 3637–3648

[16] Van Den Bout, D.E., Miller, T.K.: 'Graph partitioning using annealed neural networks', *IEEE Trans. Neural Netw.*, 1990, **1**, (2), pp. 192–203

[17] Zhao, Q., Sun, K., Zheng, D.-Z., *et al.*: 'A study of system splitting strategies for island operation of power system: A two-phase method based on OBDDs', *IEEE Trans. Power Syst.*, 2003, **18**, (4), pp. 1556–1565

[18] Sun, K., Zheng, D.-Z., Lu, Q.: 'Splitting strategies for islanding operation of large-scale power systems using OBDD-based methods', *IEEE Trans. Power Syst.*, 2003, **18**, (2), pp. 912–923

[19] Sun, K., Zheng, D.-Z., Lu, Q.: 'A simulation study of OBDD-based proper splitting strategies for power systems under consideration of transient stability', *IEEE Trans. Power Syst.*, 2005, **20**, (1), pp. 389–399

[20] Xu, G., Vittal, V., Meklin, A., *et al.*: 'Controlled islanding demonstrations on the WECC system', *IEEE Trans. Power Syst.*, 2011, **26**, (1), pp. 334–343

[21] Trodden, P.A., Bukhsh, W.A., Grothey, A., *et al.*: 'Optimization-based islanding of power networks using piecewise linear AC power flow', *IEEE Trans. Power Syst.*, 2013, **29**, (3), pp. 1212–1220

[22] Patsakis, G., Rajan, D., Aravena, I., *et al.*: 'Strong mixed-integer formulations for power system islanding and restoration', *IEEE Trans. Power Syst.*, 2019, **34**, (6), pp. 4880–4888, doi: 10.1109/TPWRS.2019.2920872

[23] Ding, L., Gonzalez-Longatt, F.M., Wall, P., *et al.*: 'Two-step spectral clustering controlled islanding algorithm', *IEEE Trans. Power Syst.*, 2012, **28**, (1), pp. 75–84

[24] Trodden, P.A., Bukhsh, W.A., Grothey, A., *et al.*: 'Optimization-based islanding of power networks using piecewise linear AC power flow', *IEEE Trans. Power Syst.*, 2014, **29**, (3), pp. 1212–1220

[25] Trodden, P., Bukhsh, W., Grothey, A., *et al.*: 'MILP islanding of power networks by bus splitting'. 2012 IEEE Power and Energy Society General Meeting, San Diego, CA, USA, 2012, pp. 1–8

[26] Teymouri, F., Amraee, T., Saberi, H., *et al.*: 'Toward controlled islanding for enhancing power grid resilience considering frequency stability constraints', *IEEE Trans. Smart Grid*, 2017, **10**, (2), pp. 1735–1746

[27] Amraee, T., Saberi, H.: 'Controlled islanding using transmission switching and load shedding for enhancing power grid resilience', *Int. J. Electr. Power Energy Syst.*, 2017, **91**, pp. 135–143

[28] Chiang, H.-D.: '*Direct methods for stability analysis of electric power systems: theoretical foundation, BCU methodologies, and applications*' (John Wiley & Sons, Singapore, 2011)

[29] Vu, T.L., Turitsyn, K.: 'Lyapunov functions family approach to transient stability assessment', *IEEE Trans. Power Syst.*, 2015, **31**, (2), pp. 1269–1277

[30] Bosetti, H., Khan, S.: 'Transient stability in oscillating multi-machine systems using Lyapunov vectors', *IEEE Trans. Power Syst.*, 2017, **33**, (2), pp. 2078–2086

[31] Bhui, P., Senroy, N.: 'Real-time prediction and control of transient stability using transient energy function', *IEEE Trans. Power Syst.*, 2016, **32**, (2), pp. 923–934

[32] Kamali, S., Amraee, T., Bathaee, S.M.T.: 'Prediction of unplanned islanding using an energy based strategy', *IET Gener. Transm. Distrib.*, 2016, **10**, (1), pp. 183–191

[33] Kamali, S., Amraee, T., Capitanescu, F.: 'Controlled network splitting considering transient stability constraints', *IET Gener. Transm. Distrib.*, 2018, **12**, (21), pp. 5639–5648

[34] Aylett, P.: 'The energy-integral criterion of transient stability limits of power systems', *Proc. IEE-Part C, Monographs*, 1958, **105**, (8), pp. 527–536

[35] Available at https://www2.ee.washington.edu/research/pstca/pf118/pg_tca118bus.htm